The A-Dependence of J/ψ Photoproduction Near Threshold

P. Bosted (spokesperson), J. P. Chen, *E. Chudakov (spokesperson)*,* D. Gaskell
J. M. Laget

Thomas Jefferson National Accelerator Facility

J. A. Dunne (spokesperson), D. Dutta

Mississippi State University

G. Huber

University of Regina

H. Mkrtchyan, A. Asaturyan, A. Mkrtchyan, T. Navasardyan, V. Tadevosyan

Yerevan Physics Institute

W. Chen, H. Gao, X. Qian, Y. Qiang, Q. Ye, W. Z. Zheng, X.'Zong, X. F. Zhu

Triangle Universities Nuclear Laboratory Duke University

M. Christy, C. Keppel, L. Tang

Hampton University, and Jefferson Lab

D. Day

University of Virginia

K. Griffoen

College of William and Mary

E. Cisbani, F. Cusanno, F. Garibaldi, S. Frullani

INFN, Gruppo Collegato Sanita' and Istituto Superiore di Sanita'

G. M. Urciuoli

INFN, Sezione di Roma

M. Iodice

INFN, Sezione di Roma3

L. Lagamba, E. Nappi, R. De Leo, S. Marrone

INFN Sezione di Bari and University of Bari

June 20, 2007

Abstract

The primary goal of this experiment in Hall C is the measurement of the A-dependence of quasi-free J/ψ photoproduction with an average photon energy near 11 GeV. Analysis of these data will permit a greatly improved determination of the fundamental J/ψ-nucleon total cross section. In order to reduce modeling uncertainties, we will also make precision measurements of the (s, t) dependence of the elementary J/ψ photoproduction cross section on the proton, improving the existing data and extending them to the threshold area. Comparisons to models will allow improved determination of the reaction mechanism.

The experiment consists of passing a 50 μA, 11 GeV electron beam through 10% r.l.-thick nuclear targets ranging from Be to Au, for the A-dependence measurements. J/ψ particles produced by real photons (using the targets themselves as radiators) and quasi-real photons from electron scattering near 0 degrees will have typical momenta of 10 GeV and angles of only a few degrees with respect to the beam axis. The J/ψ particles will be identified through their decays to $e^+ e^-$ or $\mu^+ \mu^-$ pairs (6% branching ratio each). The major part of the data will be taken with the positively-charged leptons detected in the SHMS with $P = 5.8$ GeV and $\theta = 15°$, while the negatively-charged leptons will be detected in the HMS with $P = 4.2$ GeV and $\theta = 21°$. Due to the very high transverse momenta of the leptons and the good spectrometer resolutions, backgrounds are small and very clean identification of J/ψ particles will be possible. Additional measurements with a liquid hydrogen target (preceded by a 10% r.l. radiator) will be made at several spectrometer settings with 11 GeV, 10.2 GeV and 8.8 GeV electron beam energies to measure the (s, t) dependence of the cross section in the kinematic region accessible with reasonable count rates. The resulting improvement in our knowledge of the elementary cross section is necessary to minimize systematic errors in the A-dependence measurements, due to the substantial Fermi-broadening effects. The cross section near threshold is also of theoretical interest, as the production mechanism is expected to be dominated by multiple gluon exchange.

The principal requirements beyond the planned standard Hall C configuration are for a set of nuclear targets, and an external radiator for the liquid hydrogen target. A total of 21 day is needed for data taking, with an additional 3 days needed for checkout, energy change, and configuration changes.

*contactperson, email gen@jlab.org

Contents

1 Introduction

The JLab upgrade to 12 GeV will allow the production of charmed particles close to the photoproduction threshold on free nucleons. Compared to the photoproduction of lighter vector mesons, the $c\bar{c}$ J/ψ is of particular interest. Its coupling of the nucleon is dominated by multi–gluon exchange; so it is sensitive to the gluon structure of the nucleon. This results from the heavy charm quark mass, which strongly suppresses the intrinsic charm content of the nucleon. Here, it is proposed to measure the A-dependence of the J/ψ photoproduction cross section using the 11 GeV electron beam in Hall C, incident on various nuclear targets. We aim to improve the previous measurements of the J/ψ cross sections on nuclei by more than a factor of three in both statistical and systematic precision, and to extend the measurements to lower energies. This will allow for a much improved extraction of the J/ψ-nucleon cross section. In order to reduce modeling uncertainties, we will also make precision measurements of the (s, t) dependence of the elementary J/ψ photoproduction cross section on the proton, improving the existing data and extending them to the threshold area. Comparisons to models will allow improved determination of the reaction mechanism.

1.1 Kinematics and distance scale

The close-to-threshold photoproduction of charmonium has particular features due to the kinematics of the reaction products. For J/ψ production on nucleon, the threshold energy is $E_\gamma = 8.20$ GeV and, due to the large mass of the charmed quark ($m_c \approx 1.5$ GeV), the $c\bar{c}$ fluctuation of the photon travels over $l_c \cong 2E_\gamma/4m_c^2 = 0.36$ fm (see Fig. 1). The large mass of the charmed quark also generates a small transverse size $r_\perp \sim 1/(\alpha_s m_c) = 0.3$ fm of this fluctuation. The minimum value allowed for the momentum transfer is large ($t_{min} \sim 1.7$ GeV^2 at the very threshold, ~ 1 GeV^2 at $E_\gamma = 10$ GeV). Thus charm production near threshold implies a small impact distance ($b \sim 1/m_c \sim 0.13$ fm).
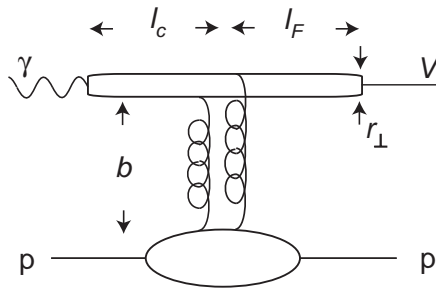

Figure 1: The characteristic time scales in J/ψ production on proton.

Close to threshold, the formation length (during which the $c\bar{c}$ pair evolves into a

J/ψ, after its interaction with a nucleon)

$$l_F \cong \frac{2E_\gamma}{m_{\psi'}^2 - m_{J/\psi}^2} \cong 0.1 E_\gamma \quad \left[\text{fm} \cdot \text{GeV}^{-1}\right] \tag{1}$$

is about 1 fm, closer to the nucleon size than the nucleus size. This is the ideal situation to determine the scattering cross section of a full-sized charmed meson on a nucleon, in contrast with higher energies which instead allow access to the nuclear interaction of a compact $c\bar{c}$ pair.

1.2 J/ψ–nucleon cross section

The dynamics of charmonia production and interaction has been a subject of interest since their discovery. Because of a small size of these heavy mesons it has been expected that perturbative QCD is applicable to calculations of the hadronic cross section.

The interest has grown further, after charmonium suppression had been suggested as a signature for the quark-gluon plasma search in relativistic heavy-ion collisions.

Since no direct measurement of J/ψ-nucleon cross section is possible, it must be extracted from other data. Various techniques have been applied:

1. using the data on elastic photoproduction of charmonia $\gamma p \to J/\psi p$ in a framework of Vector Dominance model (VDM), along with optical theorem and certain assumptions on the ratio of real and imaginary parts of the scattering amplitude;

2. using the A-dependence of the photo and hadro-production cross section, with the help of nuclear scattering models, like the Glauber model.

The first result obtained from the method 1 came from SLAC [1] $\sigma_{tot}^{\psi N} \approx 1$ mb, while the A-dependence measurement (method 2) at SLAC at 20 GeV [2] gave a value of $3.5 \pm 0.8 \pm 0.5$ mb. The first estimates of $\sigma_{tot}^{\psi N}$ derived from J/ψ hadroproduction, gave a value of ≈ 7 mb [3]. Since then, a number of corrections have been made for both methods.

For method 1 it was argued [4] that the VDM should be extended to a multi-channel case, which provided a value of $\sigma_{tot}^{\psi N} \approx 2.8 - 4.1$ mb instead of 1 mb. In another attempt [5,6] to use the photoproduction results to extract $\sigma_{tot}^{\psi N}$, the short-distance QCD and the gluon PDF of nucleons were applied to reproduce the experimental results on J/ψ photoproduction. Then, a combination of the VDM, the optical theorem and dispersion relations yielded a prediction of $\sigma_{tot}^{\psi N} \sim 0.3$ mb for the SLAC energies, most likely a strong underestimation.

Method 2 was reconsidered taking into account possible color transparency effects [7, 8, 9, 10] and it was concluded that at low energy photoproduction the color transparency did not make a sizable contribution, and that the SLAC results at 20 GeV were reliable. At higher energies it may not be the case. The results of J/ψ hadroduction have been also reconsidered taking in account energy loss of the beam particle and quantum coherence effects, and a value of $\sigma_{tot}^{\psi N} \approx 3.6$ mb was obtained, instead of 7 mb.

On the other hand, it has been argued [11] that in hadronic interactions at high energy various charmonium states are produced, which eventually decay to J/ψ. This may shift the effective J/ψ absorption rate.

Thus, the extraction of $\sigma_{tot}^{\psi N}$ has created a considerable experimental and theoretical confusion. One may conclude that the low energy data on A-dependence of photo-production play the most important role in deriving the $\sigma_{tot}^{\psi N}$ cross section, providing a measurement not calling so far for strong subsequent corrections. Only one such measurement has been done in the range considered nearly free from possible color transparency corrections - at 20 GeV [2]. However, that data have many limitations. The signal was obtained by subtraction of a large calculated background, and no information on the J/ψ kinematics was available. Therefore the signal included both coherent and incoherent contributions. Only two targets were compared. All this calls for a new measurement, and 10–11 GeV at JLab is the perfect energy range. The photoproduction cross section, measured at 11 GeV [12] as ~ 0.5 nb, is sufficiently large. Both the coherence length $l_c \cong 2E_\gamma/4m_c^2 \approx 0.5$ fm and the formation length $l_F \approx 1$ fm are half of those of the SLAC experiment and are smaller than the nucleus size. This minimizes the color transparency effects. At 11 GeV one may expect a steeper energy dependence of the cross section, than at 20 GeV, which may require larger corrections due to the Fermi motion. It will be demonstrated that this effect is under control. The total J/ψ–nucleon cross section $\sigma_{tot}^{\psi N}$ will be measured at $\sqrt{s} \sim 5$ GeV, which is in the range of interest for the quark-gluon plasma studies.

1.3   J/ψ photoproduction close to threshold

Both for extracting the J/ψ–nucleon cross section and for the interpretation of the results we must know the J/ψ photoproduction differential cross section on free nucleons. One expects that the cross section falls rapidly with the photon energy approaching the threshold. Both the energy and the t–dependence characterizes the reaction mechanism. The existing experimental data below ~ 15 GeV are very limited and contradict each other. The measurement at the lowest energy of 11 GeV [12] published a t-slope of ~ 1.1 (GeV/c)$^{-2}$), which seems not to match their own raw t-distributions, and is very different from the slope of ~ 2.9 (GeV/c)$^{-2}$, measured at 20 GeV [1]. The results on the cross section energy dependence at 11 GeV are also confusing, hinting at possible large cross section closer to threshold.

Jefferson Lab is the unique place to make precise measurements of of J/ψ photoproduction below 11 GeV, where it probes the gluon generalized distributions at high values of x.

2   Experiment

The A-dependence of the J/ψ production cross section can be affected by several effects, different from the J/ψ interaction in nuclear matter. The observed rate of J/ψ is the

date	reference	experiment	beam	energy	target	state
1975	Knapp [13]	FNAL	γ	50–200 GeV	Be	J/ψ
1975	Gittelman [12]	Cornell	γ	11 GeV	Be	J/ψ
1975	Camerini [1]	SLAC	γ	13–21 GeV	p, d	J/ψ, ψ'
1976	Nash [14]	FNAL	γ	31–80 GeV	d	J/ψ
1976	Andersen [15]	SLAC	γ	9.5-15 GeV	Be, Ta	J/ψ
1982	Binkley [16]	FNAL	γ	60–300 GeV	p, d	J/ψ
1984	Denby [17]	FNAL	γ	105 GeV	p	J/ψ
1986	Sokoloff [18]	FNAL E691	γ	120 GeV	p, Be, Fe, Pb	J/ψ
1987	Barate [19]	CERN NA14	γ	90 GeV	^{6}Li	J/ψ, ψ'
1993	Frabetti [20]	FNAL E687	γ	100–375 GeV	Be	J/ψ
1997	Breitweg [21,22]	HERA ZEUS	e	850–32400 GeV	p	J/ψ
2000	Aldoff [23,24]	HERA H1	e	360–43300 GeV	p	J/ψ, ψ'

Table 1: Summary of experimental measurements of J/ψ photoproduction.

result of a convolution of the photon energy spectrum, the Fermi motion (which changes the center-of-mass energy), the energy dependence of the production cross section and the detector acceptance.

2.1 J/ψ photoproduction cross section

In order to extract $\sigma_{tot}^{\psi N}$ from the A-dependence of the J/ψ yields, one needs to know the energy dependence of J/ψ photoproduction on the nucleon.

2.1.1 Experimental data

Several experiments have been done at different photon energies, starting with 11 GeV, many of them used nuclear targets (see Table 1).

Two processes contribute to the photoproduction on nuclei:

1. coherent production on the nucleus $\gamma A \to J/\psi A$ is characterized by a large t-slope of $b \sim 30$ (GeV/c)$^{-2}$;

2. incoherent production on nucleons $\gamma N \to J/\psi X$ is characterized by a small t-slope $b \sim 2$ (GeV/c)$^{-2}$.

One can also distinguish two processes contributing to photoproduction on free nucleons:

1. "elastic" production $\gamma N \to J/\psi N$;

2. "inelastic" production $\gamma N \to J/\psi X$, where additional particles (pions) are produced.

In many of the experiments the "elastic" production $\gamma N \to J/\psi N$ was not separated from the inelastic one $\gamma N \to J/\psi X$. The relative inelastic contribution was measured at $60 < E_\gamma < 300$ GeV on hydrogen as $30 \pm 4\%$ [16]. For the production on nuclei at $E_\gamma > 50$ GeV, the $\frac{d\sigma}{dt}$ differential cross sections clearly demonstrates a considerable contribution (up to $\sim 50\%$) of the coherent production $\gamma A \to J/\psi A$ [14, 18, 19, 20]. In order to select only the incoherent production, a cutoff of about $t < -0.15$ $(\mathrm{GeV/c})^2$ was used [18]. The measured differential cross sections of $\gamma N \to J/\psi X$ have been described using a conventional parametrization:

$$\frac{d\sigma}{dt}(E_\gamma) = \sigma_\circ(E_\gamma) \exp\left(b(E_\gamma)t\right) \tag{2}$$

where $t = (p_\psi - p_\gamma)^2$. In order to extract the photoproduction cross section on nucleon we assume temporarily that $\sigma_{\gamma A} = A \cdot \sigma_{\gamma N}$. The results of several low energy measurements are summarized in Table 2. The values for the full cross section σ were derived from the experimental values for $\frac{d\sigma}{dt}|_{tmin}$ as $\sigma = \frac{d\sigma}{dt}|_{tmin}/b$. There is an indication that the slope b increases with energy: $b = 1.13$ $(\mathrm{GeV/c})^{-2}$ [12][1] at 11 GeV and $b = 2.9$ $(\mathrm{GeV/c})^{-2}$ [1] at 21 GeV. On the other hand, the differential cross sections $\frac{d\sigma}{dt}|_{tmin}$ must have been calculated using the number of events observed N_{obs}, as $\frac{d\sigma}{dt}|_{tmin} \propto N_{obs} * b$. Different values for b have been used: 2.9 $(\mathrm{GeV/c})^{-2}$ [1], 2.0 $(\mathrm{GeV/c})^{-2}$ [15] and 1.13 $(\mathrm{GeV/c})^{-2}$ [12]. Therefore, we calculate $\sigma = \frac{d\sigma}{dt}|_{tmin}/b$, using the same values of b.

2.1.2 Coherent, incoherent and inelastic processes

The incoherent processes can be used for the $\sigma_{tot}^{\psi N}$ measurement, while the coherent production $\gamma A \to J/\psi A$ is a background. Coherent production is characterized by a t-dependence with a large slope. for example at $E_\gamma > 60$ GeV [18] the data were consistent with a slope $b > 30$ $(\mathrm{GeV/c})^{-2}$, while the coherent contribution for lead, corrected for $|t_{min}|$, was about 1.1 of the incoherent contribution. For 11 GeV a large $|t_{min}| \approx 0.2$ $(\mathrm{GeV/c})^2$ provides a suppression of the coherent part to a $\sim 0.2\%$ level.

The coherent contribution is essentially negligible. Therefore, we can center the spectrometer acceptance for J/ψ–s produced at small angles. A good experimental resolution in t (see Section 2.3.3) will allow us to put an experimental limit on the coherent contribution.

The "inelastic" production poses a potential problem for the differential cross section measurement on hydrogen. The photon energy is not directly measured, but can be reconstructed from the kinematics, for the "elastic" reactions. This issue is discussed in Section 2.6.

---

[1]Accordingly to M. Strikman, this published result contradicts the data from the same experiment. We still use the slope $b = 1.13$ $(\mathrm{GeV/c})^{-2}$ as the lower limit.

reference	E_γ GeV	target	σ nb per nucleon	$\frac{d\sigma}{dt}\big|_{t=0}$ nb/(GeV/c)^2 per nucleon	b (GeV/c)$^{-2}$
Gittelman [12]	9.0–11.0	Be	0.6 ± 0.1	0.9 ± 0.1	1.13 ± 0.18
Camerini [1]	13.0–13.5	D	1.3 ± 0.3	7.5 ± 1.6	2.9
	15.0–16.0		2.0 ± 0.3	9.4 ± 1.6	2.9
	16.0–16.5		2.8 ± 0.4	12.0 ± 1.6	2.9
	17.0–17.5		3.7 ± 0.3	15.1 ± 1.4	2.9
	19.0–19.5		4.1 ± 0.3	15.5 ± 1.4	2.9
	21.0–21.5		5.0 ± 0.4	17.8 ± 1.5	2.9
Anderson [15]†	9.5	Be/Ta	0.12 ± 0.08	–	–
	11.5		0.23 ± 0.08	–	–
	13.5		1.7 ± 0.3	–	–
	15.0		2.9 ± 0.4	–	–
Barate [19]	39.0	Li	11.2 ± 2.3	–	–

† Unpublished results

Table 2:   Measurements of the J/ψ photoproduction cross section on the nucleon at $E_\gamma < 40$ GeV. The t-slope b is presented, if measured in the given experiment.

2.1.3   Modeling the differential cross section

In order to describe the energy dependence of the "elastic" production we use a model [25]. The model takes into account that, close to threshold, the spectator partons carry a vanishing fraction $x \sim 0$ of the target momentum. The quark counting rules apply and, in case of one spectator quark, or 2-gluon exchange, the cross section would be

$$\sigma \propto (1-x)^2/(R^2\mathcal{M}^2), \tag{3}$$

where $\mathcal{M}$ is the mass of the $c\bar{c}$ pair, $R \approx 1/m_c$ is the interquark distance and $x = (2m_p\mathcal{M}+\mathcal{M}^2)/(s-m_p^2)$. Here $\sqrt{s}$ is the center of mass energy and m_p is the proton's mass. The t-dependence, driven by proton formfactors, was parametrized by an exponential $e^{b\cdot t}$. We varied the value of b between 1.1 and 2.9 (GeV/c)$^{-2}$ in order to study possible sensitivity of the rates to this parameter. After taking into account the phase space and the coupling of the incoming photon to a $c\bar{c}$ pair, one free parameter remains for the normalization of the cross section. The result of the fit to the data in a range of 9-25 GeV is shown in Fig. 2.

We also tried a different shape of the t-dependence, derived from a 2-gluon formfactor of the nucleon [26]:

$$\frac{d\sigma}{dt} \propto \frac{1}{(1-t/m_{2g}^2)^4}, \tag{4}$$

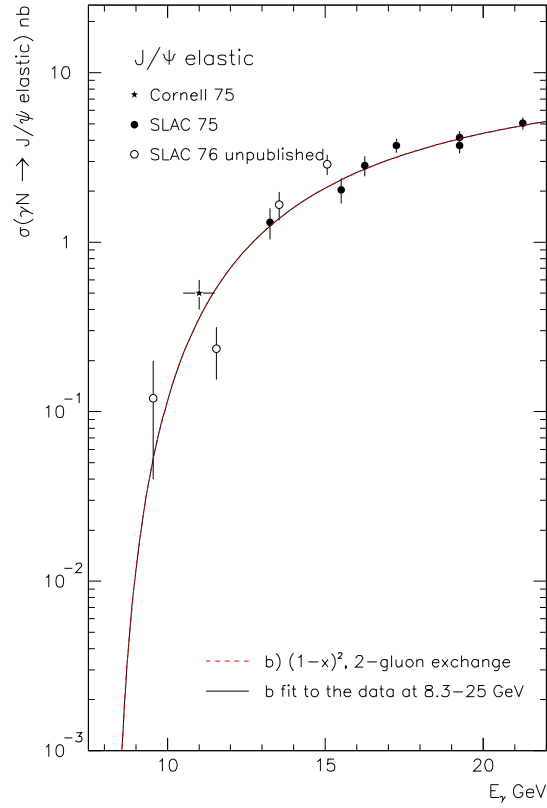where $m_{2g} = 1.1$ (GeV/c)^2 is obtained from high energy data.

Figure 2: Experimental data on J/ψ photoproduction cross section measured at low energies and the results of a model [25] fit to these data. The unpublished SLAC data were obtained in a single arm experiment, after a subtraction of the calculated background from the observed muon spectra.

2.2   Fermi Motion

In order to simulate the Fermi motion we used the spectral functions [27] for carbon, iron and lead. The function $f(|k|, E_m)$ is proportional to the probability to find a nucleon with the full momentum $|k|$ and the removal energy E_m. The energy of the struck nucleon was calculated as $k_\circ = M_A - \left[(M_A - m_p + E_m)^2 + |k|^2\right]^{1/2}$ (see [28], Eq.5). The 1-dimensional distributions for the nucleon momentum and its missing mass are shown in Fig. 3. The demonstrated difference in the average nucleon momenta for carbon and gold leads to a distortion of the A–dependence of the yields because of the steep energy dependence of the cross section.
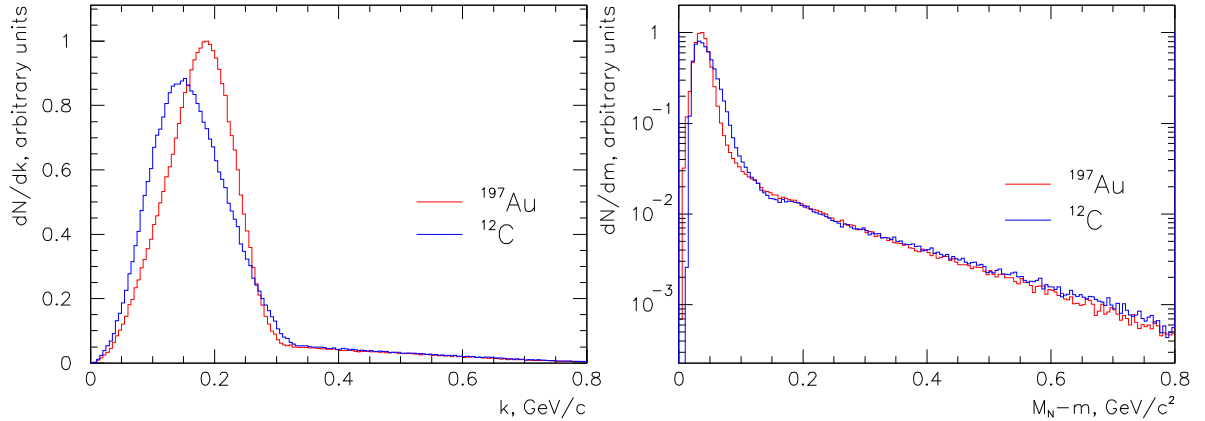
Figure 3: The distribution of the full nucleon momentum $|k|$ and its "missing mass" $m_p - m$, calculated from the spectral functions for carbon and gold.

2.3 J/ψ detection

2.3.1 J/ψ production by a Bremsstrahlung photon beam

Photons from Bremsstrahlung in the target material as well as the "internal" Bremsstrahlung from a 50 μA electron beam will be used. A simple Bremsstrahlung beam spectrum was simulated: $dN_\gamma/dE_\gamma \propto 1/E\gamma$, with an endpoint of 11 GeV. J/ψ production was simulated using Eq. 2, and the energy dependence is shown in Fig. 2. The angular distribution of J/ψ leptonic decays are simulated assuming helicity conservation: $(1 + \cos^2 \theta_{CM})$ [29]. The momenta of J/ψ and the photon energy distribution for the produced J/ψ mesons are presented in Fig. 4.
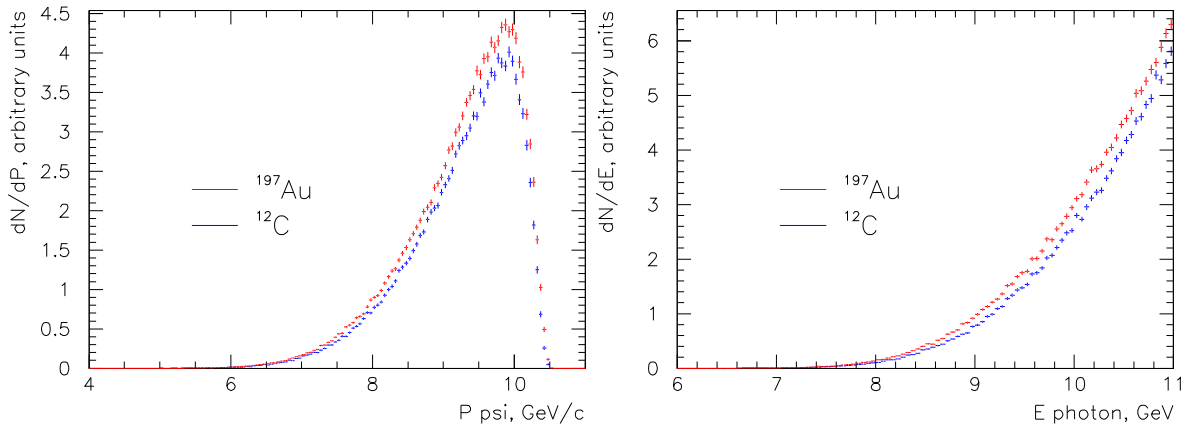

Figure 4: The distribution of the momentum of J/ψ-s produced by a Bremsstrahlung beam with endpoint energy of 11 GeV (left), and the photon energies for the J/ψ-s produced (right). Both plots are given for carbon and gold targets. The yield from gold is slightly higher than the yield from carbon because of the larger average Fermi motion.

The Fermi motion along with the production energy dependence lead to a relative increase of the rates on heavy targets: $Fe/C \approx 1.123$ and $Au/C \approx 1.134$.

2.3.2 Spectrometer settings and acceptance

The optimal momentum acceptance for J/ψ should cover a range 9.5-10 GeV, at the peak of the momentum distribution (see Fig. 4). We propose to select J/ψ-s at low P_T in order to maximize the rate, since at < 11 GeV the coherent production is small and there is no need to suppress it further by selecting high–t events (see Section 2.1.2).

The parameters of the Hall C spectrometers are shown in Table 3.

spectr.	P range GeV/c	$\Delta P/P$	$\sigma P/P$	θ^{in} range	$\Delta\theta^{in}$ mrad	$\Delta\theta^{out}$ mrad	$\Delta\Omega$ msr	$\sigma\theta^{in}$ mrad	$\sigma\theta^{out}$ mrad
HMS	0.4–7.4	$-10+10\%$	0.1%	10.5°–90°	±24	±70	8	0.8	1.0
SHMS	2.5–11.	$-15+25\%$	0.1%	5.5°–25°	±20	±50	4	1.0	1.0

Table 3: Hall C spectrometers.

The proposed settings of the spectrometers are shown in Table 4.

set	HMS		SHMS	
	θ	P, GeV/c	θ	P, GeV/c
1	21.0°	4.20	15.0°	5.80

Table 4: Spectrometer settings for nuclear targets.

The momentum distribution of the detected J/ψ mesons and the energies of the photons are shown in Fig. 5. Practically, only the events created by photons at $E_\gamma >$ 10 GeV are detected.

The relative increase of the rates on heavy versus light nuclei due to Fermi motion is slightly reduced for the detected events, to $Au/C \approx 1.09$. In order to evaluate this correction, we have to accurately model the energy dependence of the cross section on free nucleons, in the effective energy range. This range, demonstrated in Fig. 6(left) goes beyond the 11 GeV endpoint.

The acceptance for the J/ψ produced by photons in the 9–11 GeV range, with the production energy dependence shown in Fig. 2, and the t-slope $b = 1.13$ (GeV/c)$^{-2}$ (measured at ∼11 GeV [12]), is about $\epsilon \approx 0.28 \cdot 10^{-3}$ and the average cross section for the detected events is 0.29 nb. For the slope of $b = 2.9$ (GeV/c)$^{-2}$, measured at ∼20 GeV [1], the acceptance would be larger by a factor of ∼1.8. For the t-dependence of Eq. 4, the acceptance would be larger by a factor of ∼1.4.

The acceptance covers the effective masses of the detected pairs in a range of 2.8–4.1 GeV/c^2. Acceptances for e^+e^- and $\mu^+\mu^-$ decays of J/ψ are practically the same.
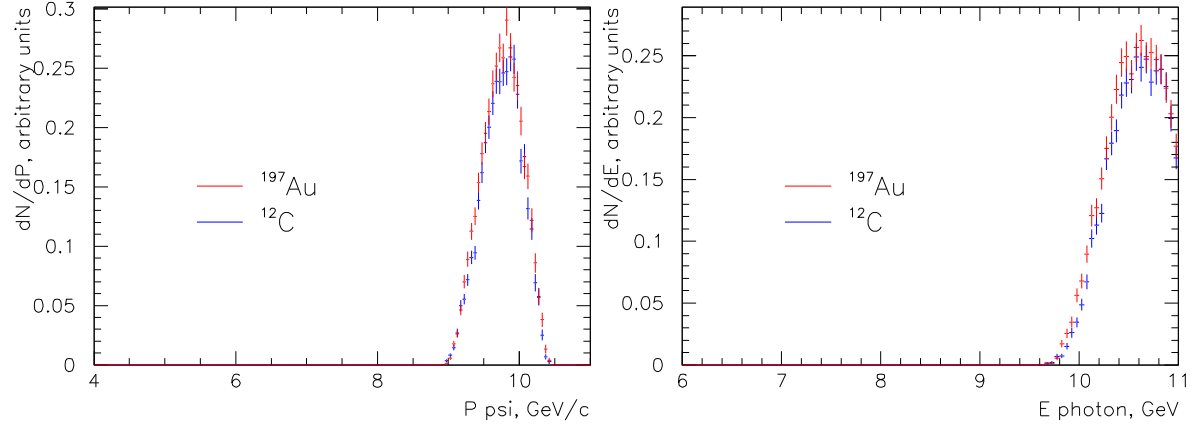
Figure 5: The distribution of the momenta of J/ψ mesons detected by the spectrometers (left), and the photon energies for the J/ψ detected (right). Both plots are given for carbon and gold targets. The yield from gold is slightly higher than the yield from carbon because of the Fermi motion.
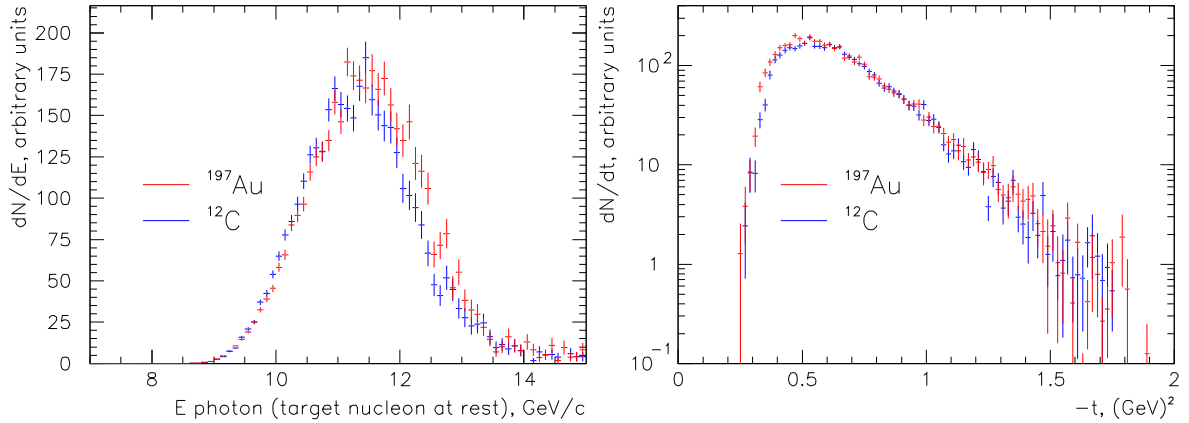

Figure 6: The distribution of the photon energies in the target nucleon rest frame (left) for the J/ψ detected, and the corresponding $-t$ distribution.

2.3.3 Resolutions

In order to minimize the multiple scattering for the secondary particles, as well as the secondary electrons' radiation, we are going to split the targets into 3 pieces, about 1 cm wide in the horizontal direction, and separated by about 5 cm in the longitudinal direction. The secondary particles will miss the downstream targets. Additionally, random coincidences will be reduced.

The mass of the J/ψ candidate is directly measured, as well as its momentum. The RMS of the mass resolution is expected to be about $\sigma_M = 7.4$ MeV/c^2, dominated by the angular resolutions of the spectrometers.

Since the production at these energies is dominated by the "elastic" process, one can reconstruct the incoming photon energy, assuming the reaction $\gamma N \to J/\psi N$. Without the Fermi motion (on hydrogen), the resolution is $\sigma_E/E \approx 0.6\%$ if no kinematic fit is done. Assigning the correct mass of J/ψ for the lepton pair and correcting the lepton momenta would improve the resolution to $\sigma_E/E \approx 0.2\%$. For the data on nuclei, the resolution becomes $\sim 2\%$.

The value of t is reconstructed in the "elastic" assumption, with an accuracy of $\sigma_t \approx 0.015$ (GeV/c)^2 with the kinematic fit.

2.3.4 Trigger

The trigger in each spectrometer will require a signal in the gas Cherenkov counter and 3 our of 4 scintillator planes. In needed, we may include the electromagnetic calorimeter with a threshold below minimum ionizing. The master trigger will be a coincidence of the trigger in each spectrometer within an approximately 100 ns wide time window.

2.3.5 Particle Identification

We will separate electron and positrons from hadron backgrounds using the gas Cherenkov and electromagnetic calorimeters in each spectrometer. These give a pion rejection factor of better than 1000:1, resulting in a negligible background from electron-hadron or hadron hadron coincidences in the mass region of the J/ψ. As in the sub-threshold experiment, we plan to identify muons by requiring a minimum ionizing signal in each layer of the electromagnetic calorimeter, and also a signal in the gas Cherenkov counter. The gas pressure will be set so that the pion threshold is 15% above the central momentum of each spectrometer. The muon threshold will then be at -15%. The muon efficiency is zero right at threshold, but rises rapidly to over 90% at -10% or so. For relative momenta above 15%, there will be be an increasingly large pion contamination. In any case, the largest source of pion contamination is from pion that decay to muons between the target and Cherenkov detector. Based on previous experience at SLAC, Fermilab, and JLab, we expect less than 10% background under the di-muon mass peak due to the good momentum and angle resolutions of the two spectrometers. This small background will be accurately subtracted using data on either side of the J/ψ mass peak.

2.4 J/ψ rates on nuclear targets

We will use various target materials, in a 50 μA electron beam. The full target thickness will be about 10% of the radiation length (T_{RL}). Without a pre-radiator, the effective luminosity of the Bremsstrahlung photons in an energy range of $E_1 - E_2$, interacting with the target, is:

$$\frac{d\mathcal{L}}{dt} = \frac{dN_e}{dt} N_{Av} \ln \frac{E_2}{E_1} \cdot T_{RL} \cdot \frac{T}{T_{RL}} \left[\frac{T}{2T_{RL}} + \alpha \right], \tag{5}$$

where t is time, $\frac{dN_e}{dt} = 3.1 \cdot 10^{14}$ s^{-1} is the electron flux, $N_{Av} = 6.02 \cdot 10^{23}$ g^{-1} is Avogadro's number, T_{RL} is the target material radiation length in g·cm^{-2}, $\frac{T}{T_{RL}}$ is the actual target thickness in radiation lengths, and $\alpha = 0.016$ is the contribution of the internal Bremsstrahlung calculated for the 11 GeV endpoint, using EPA [30]. For E_1=9 GeV, E_2=11 GeV and a gold target $\frac{T}{T_{RL}} = 0.10$ thick, the luminosity is 1550 nb^{-1}s^{-1}.

For the given target thickness of $\frac{T}{T_{RL}}$, the effective luminosity on beryllium will be about 10 times larger than the luminosity on gold.

We calculated the expected J/ψ rates as follows:

$$\frac{dN_\psi}{dt} = \frac{d\mathcal{L}}{dt} \cdot \sigma_{AV} \cdot Br \cdot \epsilon, \tag{6}$$

where t is time, $\sigma_{AV} = 0.29$ nb is the average cross section per nucleon, $\epsilon = 0.28 \cdot 10^{-3}$ is the acceptance (see Section 2.3.2), and $Br = 0.12$ is the J/ψ decay branching ratio to e^+e^- and $\mu^+\mu^-$ combined. The expected rates for different targets, along with the times, needed to accumulate 4000 detected J/ψ-s for each target, are presented on Table 5. In total, 200 hours are needed for all nuclear targets. The optimal running times for various targets depend on the actual nuclear absorption will be adjusted during the data taking.

	^{1}H	^{2}H	Be	C	Al	Cu	Ag	Au
A	1	2	9	12	27	63.5	108	197
Z	1	1	4	6	13	29	47	79
T_{RL}, g·cm^{-2}	61.28	122.0	65.19	42.70	24.01	12.86	8.98	6.28
Thickness T/T_{RL}	0.022	0.027	0.10	0.10	0.10	0.10	0.10	0.10
Detected J/ψ per h	170	340	560	370	208	112	78	55
Data taking, h	24	12	7	11	19	36	51	72

Table 5: The parameters of the targets. The expected rates and the time needed to accumulate 4000 events for each target are estimated for solid targets in setting–1 at the 11 GeV endpoint. In total, 200 hours are needed. The hydrogen target is needed for the auxiliary measurement of the cross-section energy dependence. It is planned to be used with a 7% radiator. The rate is given for the 11 GeV endpoint, in setting–1, assuming for illustration $\sigma_{\gamma A} = A \cdot \sigma_{\gamma N}$.

2.5 Background rates

2.5.1 Singles Rates

We have checked that the inclusive single particle rates are well below 500 kHz in each spectrometer, so that there should not be any problems with pile-up, multiple tracks, and dead time. Specifically, the π^+ rate in the SHMS for the 10% r.l. Be target (worst case) will be about 250 kHz using the Wiser fit to SLAC data taken at similar kinematics as the present experiment [34]. Proton, kaon, and positron rates are small in comparison. In the HMS, the π^- rates is expected to be about 60 kHz for the worst case, and the π^- rates will be about 120 kHz, for a total of 180 kHz.

2.5.2 Coincidence rates

If we assume that 10% of pions produce a gas Cherenkov signal (mainly through decays to muons, but also because of knock-on electrons and scintillator light), the trigger rate in the SHMS for the worst case will be about 25 kHz. If we assume all of the electrons plus 10% of the pions make a trigger in the HMS, the rate will be about 72 kHz. With a 100 nsec time window, the accidental coincidence trigger rate will be less than 200 Hz. Due to the selected kinematics, the rate of true election pion coincidences is expected to be much smaller. The true rate of di-lepton pairs from Bethe-Heitler production is expected to also be small, of order 10 Hz or less. For the planned DAQ capability in the 12 GeV era, the total trigger rate of less than 200 Hz will not generate any significant computer dead time, and the total data volume will be relatively small.

2.5.3 Backgrounds for J/ψ detection

For a pure photon beam, the main source of di-lepton background for di-lepton mass $M_{ll} > 1$ GeV is wide-angle Bethe-Heitler pair-production. Since this is just time re-ordered lepton-nucleon or lepton nucleus scattering, the process can be accurately predicted in QED [31,32] given a model of the form factors for lepton-nucleus, lepton-nucleon, and deep-inelastic scattering. Based on previous experiments, the total di-lepton rate will be approximately the same for Bethe-Heitler as for J/ψ photoproduction, integrated over $2.8 < M_{ll} < 4.1$ GeV, corresponding to the mass region covered by set-1.

The ratio of the e^+e^- Bethe-Heitler background to the J/ψ signal has been measured in different experiments, including the experiment at Cornell [12] at 11 GeV. In a wide mass range of $\sim$0.5 GeV/c^2 the ratio was about 15%. We will have a factor of 10 better mass resolution, allowing to reduce the background to $\sim$1.5%. The background will be well measured and its shape is predictable, therefore the error caused by its subtraction is $\ll 1\%$.

For electron-positron coincidences, additional backgrounds can come from hadron electroproduction, where the detected electron scatters from a nucleus, and the hadron or it's decay products are either an actual positron, or a hadron is mis-identified as a positron. We have examined the following cases: the hadron is a π^+ and either mis-identified as a positron ($< 10^{-3}$ probability), or decays to a muon and then positron

(negligible); the hadron is a proton and is mis-identified as a positron ($<1/1000$ probability); or the hadron is a π^0 which has a positron in it's decay (either through the Dalitz decay, or by conversion of one of the decay photons in the target or scattering chamber window). We find the background from all these sources to be less than the Bethe-Heitler background. This can be readily understood due to the high Q^2 for the electron scattering (> 5 GeV^2) and the very high transverse momentum of the positrons.

In the case of di-muon detection, we anticipate that the largest source of background will be from di-pion photoproduction, in which both pions decay to muons in the spectrometer. We will evaluate this background quantitatively using the Lund Monte Carlo PYTHIA [33] to generate di-pion events. Meanwhile, the experience of the SLAC experiment in which muons were detected in the 8 GeV and 20 GeV spectrometers, with a somewhat higher photon energy endpoint, suggests that this background will be $< 10\%$ under the J/ψ mass peak, with the good resolution of the HMS and SHMS spectrometers.

A final background will come from accidental coincidences. Accidental backgrounds were less than 10% in the Cornell and SLAC experiments, which had orders-of-magnitude worse duty factors, so that we anticipate negligible accidental rates for the present proposal. This is supported by the accidental rate of less than 1 count in four days in the entire di-lepton mass region observed in the JLab sub-threshold experiment.

2.6   J/ψ cross section measurement on hydrogen

2.6.1   Purpose

It has been demonstrated in Section 2.3.2 that the Fermi motion spectra, convoluted with the production cross section as a function of the photon energy, lead to a relative increase of the detected J/ψ yields on heavy versus light nuclei: $Au/C \approx 1.100$. This factor is sensitive to the slope $\frac{d\sigma}{dE_\gamma}|_{E_\gamma=11\ GeV}$ of the cross section. A 10% steeper slope (simulated by multiplying the cross section by a factor $1 + (E_\gamma/1.GeV - 11) \cdot 0.1$ would change the correction factor by 1% ($Au/C \approx 1.110$).

In order to evaluate this correction, we have to measure the energy dependence of the cross section, namely the slope of this dependence with an accuracy better than 0.1 GeV^{-1}.

Additionally to the energy dependence, we intend to measure the t-dependence and also the dependence on the decay angle $\cos\theta_{CM}$. Both measurements are important to minimize the model dependence of the result, as well as to help to understand the production mechanisms.

Various conditions and settings for the measurements proposed are summarized in Table 6.

2.6.2   Energy dependence

The effective photon energy range for the production on nuclei is illustrated in Fig. 6(left). The range goes beyond the 11 GeV endpoint, which is located close to the center of the distribution. We can measure the slope in a range of 10–11 GeV, and combine the results with the slope obtained at higher energies from the other data [12, 1].

The photon energy bite of the acceptance is relatively broad: ~ 1 GeV. In this range the cross section from Fig. 2 varies by a factor of $\sim$3. Averaging over the acceptance range may introduce significant systematic errors, depending on the shape of the cross section curve and the knowledge of the spectrometer acceptance. A better way is to detect the photon energy on an event basis. The photon energy reconstruction is accurate enough (see Section 2.3.3) for the "elastic" production on free nucleons. On nuclear targets, in contrast, the photon energy resolution is about 0.2 GeV. Over a 0.2 GeV interval, the cross section changes by about 20%.

The average photon energy for the detected J/ψ at setting–1 (see Table 6) is $\sim$10.6 GeV. The photon energy bite for one setting is too narrow to measure the slope, considering a strong acceptance dependence on the photon energy. Therefore, a lower momentum setting (setting–5, see Table 6) is proposed to measure the production at an average photon energy of about 10 GeV.

The momentum spectra of the J/ψ observed as well as the photon spectra are shown in Fig. 7 for both settings. For the 11 GeV endpoint, the setting–5 sample contains a sizable fraction of events produced by photons close to the endpoint.

A problem with the energy reconstruction arises from an unknown contribution of the "inelastic" production of J/ψ. This contribution was measured at $E_\gamma > 60$ GeV to be $\sim$30% of the total [16], but is expected to be much smaller at 11 GeV, which is much closer to threshold.

For setting–1 at the 11 GeV endpoint, the acceptance limits the mass M_X of the recoil baryonic state to about $M_X < 1.2$ GeV/c^2. For $M_X = 1.1$ GeV, which is just above the pion production threshold, the reconstructed photon energy is shifted by ~ -300 MeV. We propose to measure the cross section for the pure "elastic" events, selecting the reconstructed photon energies[2]. of $\mathcal{E}_\gamma > 10.7$ GeV. The average photon energy for the detected J/ψ is 10.85 GeV.

Setting–5 requires a lower endpoint energy, and we propose to use 10.2 GeV. For $M_X = 1.1$ GeV, the reconstructed photon energy is shifted by ~ -400 MeV, and we select $\mathcal{E}_\gamma > 9.8$ GeV. The average photon energy for the detected J/ψ is 10.0 GeV.

We propose to use a 20 cm long liquid hydrogen target with a $\beta = 7\%$ r.l. radiator in front. The radiator (gold or silver) will be used as a separate target for J/ψ-s production. The rate on hydrogen is calculated similarly to Eq. 5:

$$\frac{d\mathcal{L}}{dt} = \frac{dN_e}{dt} N_{Av} \ln \frac{E_2}{E_1} \cdot T_{RL} \cdot \frac{T}{T_{RL}} \left[\frac{T}{2T_{RL}} + \alpha + \beta \right], \qquad (7)$$

where T_{RL} is the hydrogen radiation length in g·cm^{-2}, $\frac{T}{T_{RL}}$ is the hydrogen target thickness in radiation lengths, and $\beta =7\%$ is the radiator thickness in radiation lengths. For

---

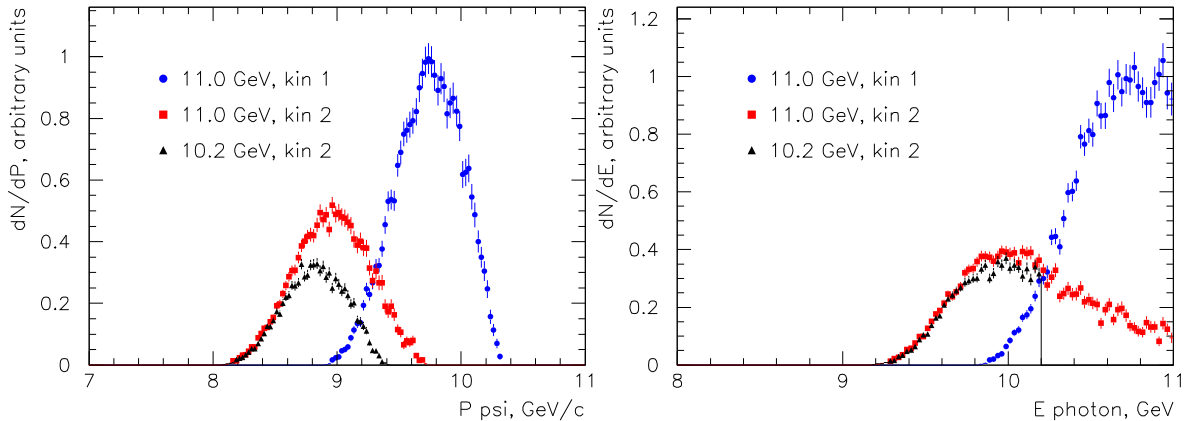[2]Here we denote the real photon energy by E_γ and the reconstructed energy by $\mathcal{E}_\gamma$

Figure 7: The distribution of the momentum of J/ψ-s detected by the spectrometers (left), and the photon energies for the J/ψ-s detected (right). Three different cases are presented, for: the 11 GeV endpoint with the high momentum setting–1, the 11 GeV endpoint with the low momentum setting–5, and the 10.2 GeV endpoint with the low momentum setting–5. The rates in setting–5 are smaller than in setting–1 because of the energy dependence of the cross section.

E_1=9 GeV, E_2=11 GeV the luminosity is 4800 nb^{-1}s^{-1}. The rates are calculated using Eq. 6 and are summarized in Table 6.

The expected J/ψ rate is $\sim$170 per hour for the 11 GeV endpoint in setting–1, while at $\mathcal{E}_\gamma > 10.7$ GeV the rate is $\sim$70 per hour. For setting–5 with the 10.2 GeV endpoint, the full rate is $\sim$60, while at $\mathcal{E}_\gamma > 9.8$ GeV the rate is $\sim$30 per hour.

The optimal ratio of running times in setting–5 versus setting–1 is about 60:40%, for the minimization of the error on the slope. To reach the statistical error of 1.5% we need to accumulate about 2000 events in setting–1 and 1400 events in setting–5, which requires 30 and 50 hours. Additional runs with the empty target have to be taken.

We measure the slope between 10 and 11 GeV, and have to extrapolate this measurement to the rest of the useful energy range of 11–12 GeV. In the model used, the former slope is 0.24 GeV^{-1}, while the latter is 0.35 GeV^{-1}. Variations of the second derivative of the curve is limited by existing data. Fitting various smooth curves to the data gave slope difference variations within ± 0.05 GeV^{-1}. We conclude that the corresponding error on the Au/C correction factor should be $< 0.5\%$.

The energy dependence measurement taken on hydrogen is done close to the endpoint, while the data on nuclei are smeared by the Fermi motion and cover a broader range 10–13 GeV of the effective photon energies (see Fig. 6). The nuclear data may include a larger "inelastic" contribution, than the hydrogen data, which may lead to a systematic error if the energy dependencies of the "inelastic" and "elastic" production are different. However, the "inelastic" events are suppressed by the spectrometer acceptance, by a factor of 10 at $M_X = 1.3$ GeV.

In order to evaluate the possible influence of the inelastic contribution, we propose

to do an additional measurement with the 11 GeV endpoint, in setting–5. The time needed is similar to the measurement at the 10.2 GeV endpoint, which is 50 hours. This will allow us to measure the "inelastic" contribution with a statistical accuracy of about 5% relative to the elastic strength. Should the result, contrary to expectations, be not compatible with zero, a model for the energy dependence of the inelastic contribution will have to be developed, normalized at the high energy results, the given measurement, and the kinematic constraints.

set	HMS θ	HMS P GeV/c	SHMS θ	SHMS P GeV/c	$\langle P_\psi \rangle$ GeV/c	$\langle P_t^2 \rangle$ (GeV/c)^2	$\langle \cos\theta_{CM} \rangle$	$\langle E_\gamma \rangle$ GeV	rate J/ψ per hour total	rate J/ψ per hour elas.
					$E_{e^-} = 11$ GeV					
1	21.0°	4.20	15.0°	5.80	9.7	0.08	-0.15	10.8	170	66
2	21.5°	4.00	16.3°	5.90	9.7	0.12	-0.15	10.8	106	17
3	28.0°	2.95	10.7°	7.50	9.7	0.08	-0.45	10.8	136	65
4	37.0°	1.90	8.0°	8.50	9.7	0.08	-0.65	10.8	72	40
5	23.4°	3.89	16.3°	5.30	8.9	0.08	-0.15	9.8	60	
					$E_{e^-} = 10.2$ GeV					
5	23.4°	3.89	16.3°	5.30	8.9	0.08	-0.15	10.0	60	30
					$E_{e^-} = 8.8$ GeV					
6	28.1°	3.24	19.1°	4.50	7.3	0.08	-0.15	8.7	0.70	0.70

Table 6: Proposed measurements of the J/ψ differential cross section, with the hydrogen target. The first column enumerates the spectrometers' configurations. The columns "selection" show the average parameters of the detected J/ψ. The average photon energy is calculated for the selected "elastic" events. The expected rates are calculated for the conditions described in the text. The total rate includes all the detected events, while the "elastic" rate is a sub-sample with the reconstructed photon energy sufficiently close to the endpoint.

Finally, we propose to measure the cross section very close to threshold, using the regular accelerator energy at 4 passes (setting–6 in Table 6). The expected event rate is only 0.7 per hour. Three days are needed to obtain about 50 events. In spite a large statistical error, it would be a unique measurement in a range where the largest difference of various approaches to the production occur. For example, if the $(1-x)^2$ factor in Eq. 3 is replaced by $(1-x)$, the rate will be four times larger.

2.6.3 t-slope

Kinematic setting-2 is designed to provide larger acceptance at the largest t values covered by setting-1, and to greatly increase the accessible $-t$ range, from $0.4 < -t < 1.0$ for setting-1, to $0.6 < -t < 1.6$ for setting-2. This will allow us to clearly distinguish between different models, and in particular between the single exponential dependence e^{bt} and a

dipole-like behavior $(1 - bt)^{-4}$ (see Section 2.1.3). A one day running will extend the available t-range.

2.6.4 Decay angle dependence

Assuming helicity conservation, the J/ψ decay angular distribution should be $(1 + r \cdot \cos\theta_{CM}{}^2)$, with $r \approx 1$. With settings–3 and setting–4, combined with setting–1, we will have 3 points on the curve, which will constrain the shape of curve and measure the value of r. With 1000 events for both settings (1 day in total) the statistical error is $\sigma_r \approx 0.1$.

2.6.5 Comparison with deuterium

In order to minimize the uncertainty in the isoscalarity correction (the neutron excess generally increases with A), we will measure the ratio of neutron over proton J/ψ photo-production using a deuteron target in setting-1. If the multi-gluon exchange mechanisms dominate, this ratio should be close to unity (after small corrections for deuteron Fermi motion and J/ψ absorption). Deviations from unity will be used in corrected for neutron excess in the A-dependence measurements, and will also give important clues as the to the reaction mechanism.

2.6.6 Summary for the hydrogen data taking

The proposed measurements of the cross section will take 11 days of data taking on hydrogen and a 0.5 day running on deuterium.

2.7 Determining $\sigma_{\text{tot}}^{\psi N}$ using A-dependence

2.7.1 Method

As stated earlier, the first extraction of the J/ψ-nucleon cross section was done at SLAC endpoint energy in 1975 using beryllium and tantalum targets and a Bremsstrahlung beam of 20 GeV. They used a single-arm spectrometer to measure high-p_T muons from J/ψ decays. Then using the measured ratio of the total cross sections per nucleon for Be and Ta targets and a simple optical model, they determined the J/ψ-nucleon cross section. This measurement is considered the best determination of the J/ψ-nucleon cross section from photoproduction experiments, but it suffered from a large background subtraction and the possibility of color transparency effects. For the present proposal with lower beam energy there is a higher probability that the $c\bar{c}$ is a fully formed J/ψ meson, allowing the use of a simple Glauber formalism. The basic input for this formalism is the target optical thickness,

$$T_A(\vec{\mathbf{b}}) = \int_{-\infty}^{\infty} dz \rho_A(\vec{\mathbf{b}}, z) \tag{8}$$

where ρ_A is the nuclear density and b is the impact parameter. The Glauber formalism, which relates the transparency factor $T_N(A) = \sigma_A / A\sigma_N$, is considered valid if the

formation length is less than the nuclear radius. This relationship is

$$T_N(A) = \frac{1}{A} \int d^2b \int_{-\infty}^{\infty} dz \rho_A(\vec{\mathbf{b}}, z) e^{-\sigma_{\psi N} \int_z^{\infty} dz' \rho_A(\vec{\mathbf{b}}, z')} \tag{9}$$

Therefore, measuring the transparency factors for two or more different nuclei, forming the ratio, and using the appropriate nuclear density profiles, one can extract the J/ψ-nucleon cross section.

2.7.2 Error budget

The errors for the (s, t)-dependence on the proton are dominated by statistical errors. An overall systematic error of approximately 3% to 4% will arise from uncertainties is expected to be sominated in the uncertainty in the effective photon flux, spectrometer acceptance (in particular for muons, for which it is difficult to define the acceptance with collimators), and radiative corrections to the electron-positron mass spectrum.

The overall systematic error in the A-dependence measurements will also be about 3% to 4%. For the extraction of the J/ψ-nucleon total cross section, the point-to-point (A-dependent) systematic errors are of greater concern. We except that they will be of the same order as the average statistical error of 1.5% for each nucleus. The principal sources of point-to-point systematic error are: target thickness uncertainty of up to 0.5% to 1.5% (largest for the gold target); and relative uncertainties of about 1% in the effective photon flux (due to both the uncertainty in the effective "internal" radiation length, as well as the actual radiation length of various materials versus A and Z). Other experimental systematic errors, such as difference in acceptance from target to target, computer and electronic dead time, beam position, and beam current measurements, are expected to total to about 0.5%. The systematic error in the J/ψ-nucleon cross section from the A-dependence will have a component due to (s, t) dependence of the free proton and neutron cross sections that we will constrain better than 1% from our measurements on proton and deuteron targets.

It is not possible to precisely quantify the theoretical error in the extraction due to effect due as Color Transparency, but we have minimized this correction by using the lowest practical photon beam energy. We plan to set some limits on the possible deviations from the Glauber model by dividing the data into three bins in reconstructed t with roughly equal statistical errors. Any significant t dependence to the extracted J/ψ-nucleon cross section could call into question the assumed extraction method. Advances in theoretical understanding of J/ψ production and propagation will be essential in the ongoing interpretation of the data from this experiment, which will provide the benchmark data set for near-threshold photoproduction.

2.7.3 Expected results

The expected nuclear transparencies and the measurement errors are shown on Table 7.

$\sigma_{\mathrm{tot}}^{\psi N}$		\multicolumn{6}{c}{A}	$\delta(\sigma_{\mathrm{tot}}^{\psi N})$
mb		9	12	27	63	108	197	mb
	1.0	0.982	0.980	0.974	0.963	0.952	0.931	0.29
T	3.5	0.938	0.931	0.908	0.870	0.833	0.760	0.25
	7.0	0.876	0.863	0.816	0.740	0.665	0.519	0.18

Table 7: The calculated nuclear transparencies for three different values of $\sigma_{\mathrm{tot}}^{\psi N}$ in a simple eikonal model, used in the SLAC experiment [2]. The errors on the derived $\sigma_{tot}^{\psi N}$ were obtained assuming a total 3% error for each point.

The expected accuracy of the measurement will be about 3 times better than the accuracy of the SLAC experiment [2]. Additionally, the interpretation of the results will be more certain because of the shorter coherence and formation lengths.

3   Technical Participation of Research Groups

3.1   Mississippi State University

One of the co-spokespeople is part of the Mississippi State University medium energy nuclear physics group. The MSU groups intends to take responsibility for the design and commissioning of the collimator and sieve-slit mechanism for the SHMS spectrometer. The MSU group is actively seeking DOE funding for this project and has already received funding for a student to work on the project. The MSU group will also develop a TRD detector program (not part of the baseline equipment) for the SHMS.

3.2   Hampton University

The Hampton University group is part of a MRI grant proposal to NSF and will be responsible for the drift chambers for the SHMS.

3.3   Yerevan Physics Institute

The Yerevan group is actively involved in this proposal and this group intends to design and build the lead-glass calorimeter for the SHMS. They will also contribute to the muon pair detection work.

4   Run plan and requests

4.1   Manpower

The collaboration has a large overlap with the approved pion CT experiment, which uses a very similar experimental setup. The collaboration also has a large overlap with the sub-threshold experiment, providing the experience to accurately simulate the present proposal.

4.2   Request

We request a total of 9 days for measurements of the A-dependence, and 12 days for measurements of of the elementary cross section on hydrogen and deuterium, necessary for the interpretation of the A-dependence. Of these, we request 2 days at the non-standard beam energy of 10.2 GeV, and 3 days at 4 passes (8.8 GeV). The remainder of the experiment at 11 GeV. We request 1 day for checkout and calibrations, and the expected overhead time is 2 days (dominated by 1 day for energy changes, with the remainder for frequent target changes to minimize systematic errors, and two spectrometer setting changes).

5   Summary

This experiment will provide definitive measurements of J/ψ photoproduction on hydrogen in the near threshold region, which will place strong constraints on the production models. Armed with this information, we can greatly improve the knowledge of the A-dependence of the elastic J/ψ photoproduction, leading to a factor-of-three better determination of the the J/ψ-nucleon total scattering cross section, a fundamental quantity that is not only calculable in specific models, but is also of practical importance in the interpretation of J/ψ suppression in heavy ion collisions.

References

[1] U. Camerini et al. Photoproduction of the psi particles. *Phys. Rev. Lett.*, 35:483, 1975.

[2] R. L. Anderson et al. A measurement of the A-dependence of psi photoproduction. *Phys. Rev. Lett.*, 38:263, 1977.

[3] C. Gerschel and J. Hufner. Comparison of J/Psi suppression in photon, hadron and nucleus nucleus collisions: Where is the quark gluon plasma ? *Z. Phys.*, C56:171–174, 1992.

[4] J. Hufner and B. Z. Kopeliovich. J/psi n and psi' n total cross sections from photoproduction data: Failure of vector dominance. *Phys. Lett.*, B426:154–160, 1998.

[5] D. Kharzeev and H. Satz. Quarkonium interactions in hadronic matter. *Phys. Lett.*, B334:155–162, 1994.

[6] D. Kharzeev, H. Satz, A. Syamtomov, and G. Zinovjev. J/psi photoproduction and the gluon structure of the nucleon. *Eur. Phys. J.*, C9:459–462, 1999.

[7] G. R. Farrar, L. L. Frankfurt, M. I. Strikman, and H. Liu. Color transparency and charmonium photoproduction. *Phys. Rev. Lett.*, 64:2996–2998, 1990.

[8] G. R. Farrar, L. L. Frankfurt, M. I. Strikman, and H. Liu. Charmonium production on nuclear targets. *Nucl. Phys.*, B345:125–136, 1990.

[9] B. Z. Kopeliovich and B. G. Zakharov. Quantum effects and color transparency in charmonium photoproduction on nuclei. *Phys. Rev.*, D44:3466–3472, 1991.

[10] O. Benhar, B. Z. Kopeliovich, C. Mariotti, N. N. Nicolaev, and B. G. Zakharov. Why photoproduction of charmonium on nuclei does not measure the charmonium nucleon total cross-section. *Phys. Rev. Lett.*, 69:1156–1159, 1992.

[11] L. Gerland, L. Frankfurt, M. Strikman, Horst Stoecker, and W. Greiner. J/psi production, chi polarization and color fluctuations. *Phys. Rev. Lett.*, 81:762–765, 1998.

[12] B. Gittelman et al. Photoproduction of the psi (3100) meson at 11-gev. *Phys. Rev. Lett.*, 35:1616, 1975.

[13] B. Knapp et al. Photoproduction of narrow resonances. *Phys. Rev. Lett.*, 34:1040, 1975.

[14] T. Nash et al. Measurement of J/psi (3100) photoproduction in deuterium at 55-gev. *Phys. Rev. Lett.*, 36:1233, 1976.

[15] R. L. Anderson. Excess muons and new results in psi photoproduction. (SLAC-PUB-1741), 1976. Invited talk presented at Int. Conf. on Production of Particles with New Quantum Numbers, Wisconsin U., Madison, Apr 22-24, 1976.

[16] M. Binkley et al. J/psi photoproduction from 60-gev/c to 300-gev/c. *Phys. Rev. Lett.*, 48:73, 1982.

[17] B. H. Denby et al. Inelastic and elastic photoproduction of J/psi (3097). *Phys. Rev. Lett.*, 52:795, 1984.

[18] M. D. Sokoloff et al. An experimental study of the A-dependence of J/psi photoproduction. *Phys. Rev. Lett.*, 57:3003, 1986.

[19] R. Barate et al. Measurement of J/psi and psi-prime real photoproduction on li-6 at a mean energy of 90-gev. *Z. Phys.*, C33:505, 1987.

[20] P. L. Frabetti et al. A measurement of elastic J/psi photoproduction cross- section at fermilab e687. *Phys. Lett.*, B316:197–206, 1993.

[21] J. Breitweg et al. Measurement of inelastic J/psi photoproduction at HERA. *Z. Phys.*, C76:599–612, 1997.

[22] J. Breitweg et al. Measurement of elastic J/psi photoproduction at HERA. *Z. Phys.*, C75:215–228, 1997.

[23] S. Aid et al. Elastic and inelastic photoproduction of J/psi mesons at HERA. *Nucl. Phys.*, B472:3–31, 1996.

[24] C. Adloff et al. Elastic photoproduction of J/psi and Upsilon mesons at HERA. *Phys. Lett.*, B483:23–35, 2000.

[25] S. J. Brodsky, E. Chudakov, P. Hoyer, and J. M. Laget. Photoproduction of charm near threshold. *Phys. Lett.*, B498:23–28, 2001.

[26] Leonid Frankfurt and Mark Strikman. Two-gluon form factor of the nucleon and j/psi photoproduction. *Phys. Rev.*, D66:031502, 2002.

[27] O. Benhar, A. Fabrocini, S. Fantoni, and I. Sick. Spectral function of finite nuclei and scattering of GeV electrons. *Nucl. Phys.*, A579:493–517, 1994.

[28] O. Benhar, S. Fantoni, and G. I. Lykasov. On the behaviour of the nuclear spectral function at high momentum and removal energy. *Eur. Phys. J.*, A5:137–141, 1999.

[29] K. Schilling, P. Seyboth, and Guenter E. Wolf. On the analysis of vector meson production by polarized photons. *Nucl. Phys.*, B15:397–412, 1970.

[30] V. M. Budnev, I. F. Ginzburg, G. V. Meledin, and V. G. Serbo. The two photon particle production mechanism. physical problems. applications. equivalent photon approximation. *Phys. Rept.*, 15:181–281, 1974.

[31] Yung-Su Tsai. Pair production and bremsstrahlung of charged leptons. *Rev. Mod. Phys.*, 46:815, 1974.

[32] Yung-Su Tsai. Pair production and bremsstrahlung of charged leptons. (erratum). *Rev. Mod. Phys.*, 49:421–423, 1977.

[33] Torbjorn Sjostrand, Stephen Mrenna, and Peter Skands. Pythia 6.4 physics and manual. *JHEP*, 05:026, 2006.

[34] David E. Wiser. *Inclusive photoproduction of protons, kaons, and pions at SLAC energies.* PhD thesis, U. of Wisconsin, 1977. UMI 77-19743.